Eur Biophys J (2010) 39:1043–1049
DOI 10.1007/s00249-009-0434-0

ORIGINAL PAPER

pH-driven helix rotations in the influenza M2 H^+ channel: a potential gating mechanism

Hadas Leonov · Isaiah T. Arkin

Received: 18 January 2009 / Revised: 16 February 2009 / Accepted: 23 February 2009 / Published online: 3 April 2009

Abstract The pH activated M2 H^+ channel from influenza A has been a subject of numerous studies due to following: (1) It serves as a target for the aminoadamantane drugs that block its channel activity. (2) M2's small size makes it amenable to biophysical scrutiny. (3) A single histidine residue is thought to control the pH gating of the channel. Recent FTIR analysis proposed that the helices of the channel rotate about their directors during pH activation. Herein, we report on molecular dynamics simulations of the X-ray structure of the protein with three charged histidine residues, representing the open form of the protein and two rotated forms with neutral histidines, representing its closed form. We compare the channel stability, convergence, interaction with water and hydration of the histidine residues that have been implicated in channel gating. Taken together, we show that both forms of the protein are stable during the course of the MD simulation and that indeed a rotation of the helices leads to channel closure. Finally, we propose a mechanism for channel gating that involves protonation of the histidine residues that necessities their increased solvation.

Keywords Ion channel · Influenza · Protein structure · Molecular dynamics · M2 channel

Viral membrane proteins, Heidelberg, December 2008.

H. Leonov · I. T. Arkin (✉)
Department of Biological Chemistry, The Alexander Silberman Institute of Life Sciences, The Hebrew University of Jerusalem, Edmund J. Safra Campus Givat-Ram, 91904 Jerusalem, Israel
e-mail: arkin@huji.ac.il

H. Leonov
e-mail: hleonov@cc.huji.ac.il

Introduction

M2 is a bitopic membrane protein that is essential for the infectivity cycle of the influenza virus. The virus inserts into the host via endocytotic uptake, where the M2 channel enables the release of viral RNA into the host cell. M2 is a homotetrameric protein with a transmembrane region that forms a pH-activated H^+ channel (Pinto et al. 1992; Sakaguchi et al. 1997). When the endosome is acidified, histidine residues in the transmembrane region of M2 become protonated, leading to the opening of the M2 channel and to a proton influx from the endosome into the virus interior (Wang et al. 1995). The acidification of the virus interior enables the release of the viral RNA into the host's cytoplasm after membrane fusion has taken place. The replication of the influenza A virus can be stopped by inhibiting the activity of the M2 channel, using antiviral agents such as amantadine, thereby making M2 an important drug-target (Hay et al. 1985, 1979).

Two theories have been brought forth to explain the conductivity mechanism of the channel: gating (Sansom et al. 1997) and shuttling (Sakaguchi et al. 1997). In the gating mechanism, water molecules penetrate the pore and form a continuous proton wire that enables the conductance (Brewer et al. 2001). The His37 residues are thought to protonate at low pH (5.5–6.0) and control the gating due to their side-chains repulsion. In the shuttling mechanism, the histidines are directly involved in the proton transfer mechanism through tautomerization or an imidazole ring flip (Lear 2003).

An experimentally derived structure of M2 based on solid-state NMR data (ssNMR) was published in the year 2002 (Nishimura et al. 2002). In an attempt to determine the channel's mechanism, various computational studies were performed on the ssNMR structure to explore its

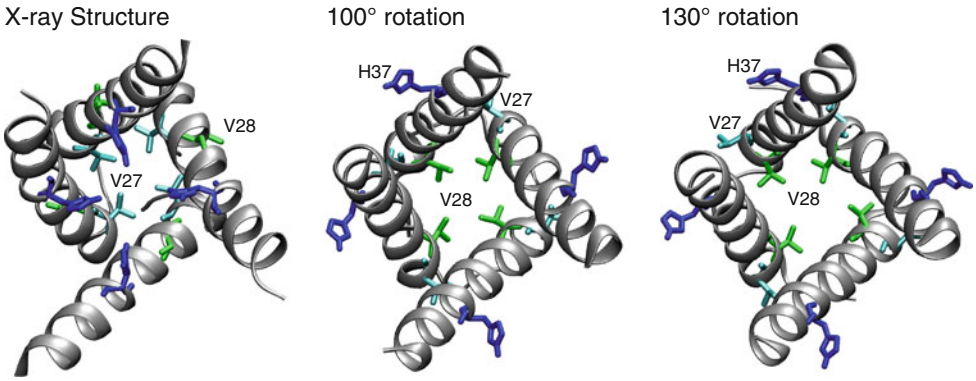

Fig. 1 A ribbon diagrams of the X-ray structure (Stouffer et al. 2008) and the two rotated structures, as indicated. Val27, Val28 and His37 are shown as indicated in the graph

dynamics, gating mechanism, ion selectivity and inhibitor binding properties (Yi et al. 2008; Chen et al. 2007; Kass and Arkin 2005; Wu and Voth 2005; Im et al. 2003).

Recently, two more experimental structures of M2 have emerged (both in detergent micelles): an X-ray structure by DeGrado and colleagues (Stouffer et al. 2008), and a solution NMR structure by Chou and colleagues (Schnell and Chou 2008).

In a recent FTIR spectroscopic study, the angles between ten isotopically labeled C=O groups and the membrane normal were measured for the M2 channel at low and high pH (Manor et al. 2009). At low pH when the channel is open, the measured angles were in very good agreement with the observed angles of the ssNMR and X-ray structures (Nishimura et al. 2002; Stouffer et al. 2008). However, at high pH when the channel is closed, the angles change significantly indicating the protein underwent a conformation change.

Rigid body modeling of a single helix of the M2 structure based on the orientational data derived from the FTIR study at low pH (Manor et al. 2009), was able to produce a model of the protein that was indistinguishable from the ssNMR and X-ray structures (Nishimura et al. 2002; Stouffer et al. 2008). However, modeling based on the FTIR data collected at high pH, resulted in a different structure. While the two structures shared the same helix tilt angle, they differed by their rotation about the helix axis by roughly 129°.

2D IR linewidths analysis in the same study, pointed towards a structural change of the channel in the pH switch, as well (Manor et al. 2009). 2D IR linewidths revealed that the accessibility of water to individual amino acids in the pore oscillates similarly in high and low pH, but the phase is shifted by one residue (i.e. 100°). This lead to an interpretation that the pore may go through a conformational change, so that it is lined with a different set of residues in each conformation, especially in its N-terminal transmembrane region (Leu26–Ala30).

Taken together, both linear and 2D IR spectroscopy have independently suggested that the channel helices rotate by 100°–129° upon pH activation. The rotation makes His37, among other residues, turn towards the helix–lipid interface. Such configuration leads to the following questions: first, how does histidine, a potentially charged amino acid, reside in the lipid interface? Second, how is histidine connected to the gating mechanism of the channel if it is buried within the lipids? Third, what makes it rotate in order to face the pore?

In this study, we use molecular dynamics (MD) to simulate the assumed open and closed forms of the channel according to the above hypothesis, in an attempt to answer some of these questions. We use the X-ray structure in a tri-protonated form to simulate an open channel. In order to simulate a closed channel, the histidines protonation state is modified to be neutral, and each of the channel's helices is rotated about its axis by either 130° or by a 100° about their axes as shown in Fig. 1. Analyses of these systems in terms of stability, convergence, water conductivity and histidine hydration is consistent with the channel state.

Materials and methods

Initial simulation setup

The initial structures used in this study were derived from the experiential X-ray structure, solved in octyl-β-D-glucopyranoside micelles, at pH 7.3, PDB code: 3BKD (Stouffer et al. 2008). It was used to generate three initial structures: (1) A tri-protonated channel that is formed when three out of four His37 residues are charged, emulating an open channel (Hu et al. 2006). (2 and 3) Two structures in which the helices are rotated by 100° or 130° about their director, representing a closed form of the channel according to (Manor et al. 2009).

The principal axis of the helical bundle was aligned to the bilayer normal, and the proteins were embedded in a pre-equilibrated dimyristoylphosphocholine (DMPC) bilayer. The bilayers initially had 128 lipids embedded in 3,687 molecules of SPC water (Berendsen et al. 1987). Colliding lipids were removed in range of 1 Å of the protein. After the

automatic removal of lipids, a visual inspection was performed, and lipids that clashed with the structure were manually removed. The original PDB contained crystal water molecules that were kept during the simulation. However, they appeared only as oxygen atoms, therefore, hydrogen atoms were added. In addition, the residues of Selenomethionine were changed to Methionine. Finally, in order to neutralize the system charge for the electrostatic calculations, Na^+ counter-ions randomly replaced water molecules in the system. The number of counter-ions was determined according to the overall charge of the channel. For the neutral closed channel, four Na^+ ions were added, whereas for the tri-protonated open channel, one Na^+ ion was added.

Energy minimization and positional restraints

Each protein system underwent energy-minimization with the conjugate gradient algorithm and a tolerance of 500 kJ mol^{-1} nm^{-1}, followed by a minimization with the Broyden–Fletcher–Goldfarb–Shanno algorithm using a slightly reduced tolerance of 300 kJ mol^{-1} nm^{-1}.

In order to prevent significant perturbations when moving from the positional restrained system to full MD where the atoms move freely, we used a gradual positional restraints (PR) procedure. In the procedure, the force constant constraining the protein and lipid atoms was gradually decreased from 1,000 to 0 kJ mol^{-1} nm^{-2}.

Two positional restraints protocols were attempted. For the open channel, both lipid and protein restraints were decreased in parallel. the procedure began by restraining the atoms using a harmonic restraint, with a force constant of $k = 1000$ kJ mol^{-1} nm^{-2} for 20 ps. Subsequent PR steps were run with a lower force constant while linearly increasing the simulation time to 100 ps at $k = 0$ kJ mol^{-1} nm^{-2}. Furthermore, the force constant was decreased by a smaller step size when the force became less stringent, starting with a step size of $\Delta k = 10$, continuing with a step of $\Delta k = 5$ at $k = 200$ kJ mol^{-1} nm^{-2} and decreasing to $\Delta k = 1$ from $k = 100...0$ kJ mol^{-1} nm^{-2}.

For the closed channel, a shorter PR procedure was applied. First, the protein was restrained while the lipid atoms restraints were decreased from 1,000 to 0 kJ mol^{-1} nm^{-2} by steps of $\Delta k = 20$. This step enabled the solvation of the protein within the bilayer, so that the lipids could close the gap created during the removal of lipids, arranging in proper orientations around the protein. Second, the protein's restraints were decreased from 1,000 to 0 kJ mol^{-1} nm^{-2} by steps of $\Delta k = 10$. The time of each step was increased linearly as described above.

MD simulations

The different systems were subjected to a 20 ns MD trajectory. The simulations were conducted using version 3.3.1 of the GROMACS MD simulation package (Lindahl et al. 2001) employing an extended version of the united atoms GROMOS87 force field (Hermans et al. 1984). The DMPC force-field parameters were taken from (Berger et al. 1997).

All simulations were conducted using the LINCS algorithm (Hess et al. 1997) to constrain bond lengths and angles of hydrogen atoms, allowing for an integration time step of 2 fs. Atomic coordinates were saved every 10 ps. Simulations were conducted at a constant temperature of 310 K. Solvent, lipids and protein were coupled separately to a Nośe–Hoover temperature bath (Nośe 1984; Hoover 1985), with a coupling constant of $\tau = 3$ ps. The pressure was kept constant by a semi-isotropic, Parrinello–Rahman pressure coupling (Parrinello and Rahman 1981; Nośe and Klein 1983) of 1 bar, with a coupling constant of $\tau = 1$ ps. A cutoff of 1.2 nm was used for van der Waals interactions. Electrostatic interactions were computed using the PME algorithm (Darden et al. 1993), with a 1.2 nm cutoff for the direct space calculation. The simulations contain approximately ~100 DMPC lipids and ~3,600 water molecules in FLEXSPC model (Berendsen et al. 1987). The total number of atoms was ~16,200. The number of atoms is not identical for all simulation systems due to the different instances of lipids and water molecules that were removed in each bilayer insertion process.

Analysis

The simulations were visualized with the Visual Molecular Dynamics (VMD) program (Humphrey et al. 1996). The analyses were conducted using in-house VMD (Humphrey et al. 1996) Tcl scripts and the GROMACS analysis package (Lindahl et al. 2001).

Results and discussion

The rotation of the helices had caused several polar residues in the protein to turn away from the pore. For example, in the 130° rotation, His37 faces the helix–lipid interface and Ser31 faces the helix–helix interface. In the 100° rotation, Ser31 is oriented more closely to the pore, and His37 is closer to the helix–helix interface, but still interacts with lipids. The rest of the polar residues such as Arginines, Aspartates and Serines are located at the edges of the helices, and turn to lipid head-groups interface mostly. Without His37 or Ser31 in the pore, most residues of the pore are hydrophobic. The C-terminus now contains a large concentration of bulky hydrophobic residues such as leucine and isoleucine.

Stability and convergence

The first element that was examined for the three different simulation systems was the stability relative to the starting

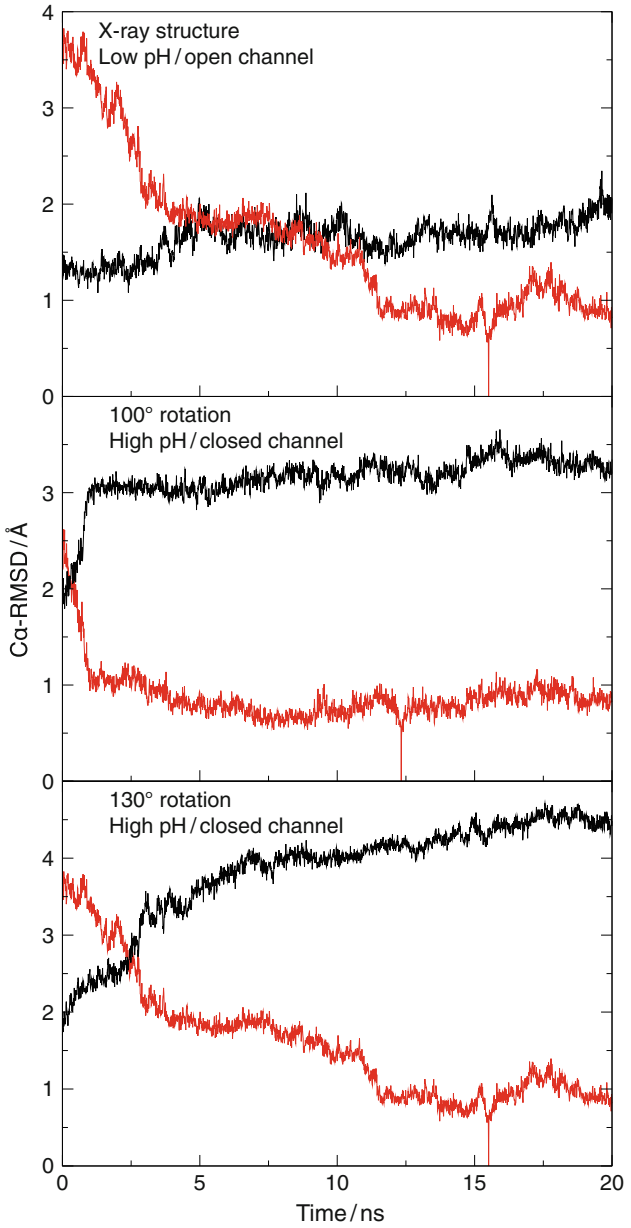

Fig. 2 Protein stability and convergence of the three systems under investigation. *Top panel*: X-ray structure with three charged histidine residues. *Middle and bottom panels*: 100° and 130° rotated structures without any charged histidines, respectively. *Dark lines* represent the Cα-RMSD of the protein as a function of time from the initial configuration. *Red lines* represent the Cα-RMSD of the protein as a function of time from the structure that best represents the outcome of the simulation

configuration as measured by a Cα-RMSD (Figure 2). The tri-protonated channel based on the X-ray structure diverged from the initial structure by ∼2 Å after 5 ns of simulation and essentially remained stable for the next 15 ns of the simulation.

The rotated, neutral channels diverged more, as expected. The channel that was rotated by 100° diverged by a Cα-RMSD of ca. 3.2 Å after 1.5 ns of simulation and remained stable throughout the duration of the simulation. Clustering of the trajectory (Cα-RMSD cutoff of 1 Å) resulted in a few small clusters, and one large cluster that stretches for the entire simulation. The average structure was found at 12.3 ns.

The channel that was rotated by 130° was less stable than the previous and diverged more from the initial structure, reaching an RMSD o 4–4.5 Å after 12 ns (Fig. 2 bottom panel). Clustering the trajectories with a 1.1 Å cutoff, indicated that nearly all structures between 12 and 20 ns belong to the same cluster that diverges from the initial structure by 4.1 Å.

The substantial differences of RMSD in the rotated structures were expected, since the initial structure of the simulation was not the X-ray structure, even though it originated from it. The rotation of the helices about their axes, changed the amino acid orientation so that the pore is mostly composed of aliphatic amino acids, while the few polar amino acids in this transmembrane region are either at the helix–helix interface, or at the helix–lipid interface. A larger rotation meant that more hydrophobic amino acids will reside in the pore, thus leading to hydrophobic interactions between helices, which in turn narrows the pore. That, in turn, resulted in a larger difference in RMSD from the initial structure. However, the structure that was rotated by 100° reached a highly stable state as indicated by the low divergence from the converged structure (Fig. 2 middle panel gray line).

Water analysis

The M2 protein is a H^+ channel, and as such it is difficult to determine explicitly the permeation probability using MD simulations. However, it is possible to track water behavior in the channel as it might facilitate proton conductivity via a Grotthus mechanism. Thus, using in-house Tcl scripts, we measured the water connectivity of the channel. Specifically, a water wire was defined as a series of water molecules connecting one side of the membrane to the other with water oxygens spaced from one another no further than 3.5 Å. In addition, we measured the diffusive permeability of the channel to water as another indirect measure of the potential of the channel to conduct protons.

The tri-protonated channel based on the X-ray structure is filled with water, especially in its C-terminal region. The N-terminal region is partially blocked due to Val27, as indicated by DeGrado and coworkers (Stouffer et al. 2008). During the dynamics of the channel, the side-chains of Val27 move so that a water-wire can sometimes be formed throughout the channel. This is more visible in simulations deriving from the bi-protonated channel, where a water wire is formed during 0.4–25% (data not shown). The tri-protonated channel does not contain such instances, but it

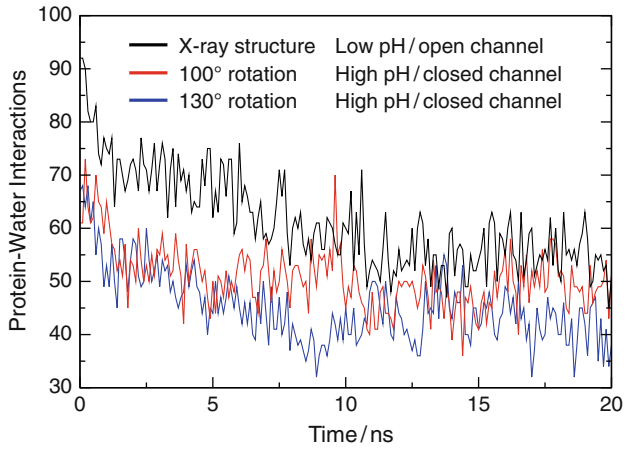

Fig. 3 Number of protein–water contacts (≤3.5 Å) that each of the different systems make. The *black*, *red* and *blue* lines represent data for the X-ray structure, 100° rotated structure and 130° rotated structure, respectively

does allow the passage of an entire water molecule on several occasions (3–4). The neutral rotated channels do not contain such instances of either water-wire formation or entire water molecule passage throughout the simulations. This is consistent with the fact that the protein should be closed at elevated pH and open at low pH (Pinto et al. 1992; Sakaguchi et al. 1997).

An analysis of water interacting with the protein during the simulations, shows a decrease of such interactions, whereby an interaction is assigned for molecules that are separated less than 3.5 Å from one another (Figure 3). In these simulations, we see a large decrease of interactions with water for all three systems. The decrease for the protonated channel is by ca. 40 water molecules, while the decrease for the neutral channels is by 25–30 water molecules.

As indicated earlier, the rotated channels present several hydrophobic pore lining residues. Where Val27 used to block the open channel (Stouffer et al. 2008), Val28 now blocks it in the same manner, at the N-terminal side. Furthermore, where His37 and Trp41 used to reside and provide the gating mechanism, there are now other bulky hydrophobic residues (Ile and Leu) that shut the pore down and make it even narrower than before, thereby minimizing the interaction with water as well.

His37 protonation is known to be connected to the gating of the channel (Wang et al. 1995; Okada et al. 2001; Takeuchi et al. 2003; Hu et al. 2006). A recent FTIR study proposed that His37 may change its rotation during pH activation. Specifically, His37 rotates such that it no longer faces the channel lumen at high pH. At low pH, when the channel opens, the His37 residues rotate along with the rest of each helix to an open channel formation, where they face the pore (Manor et al. 2009). In order for His37 to protonate, it needs to be in proximity to water molecules, which are not very common inside a lipid bilayer. However, since His37 is rather close to the C-terminal side of the transmembrane region, it is possible that its side-chain is close enough to the lipid head-groups so that sometimes water can be found near it too.

An analysis of water molecules that interact with individual histidines throughout the simulations was undertaken for each of the neutral rotated channels (Fig. 4). In the X-ray structure, taken here to represent the open channel form of the protein, the histidine residues are continuously solvated (data not shown). For the 130° rotated structure, there is at least one water molecule in proximity of 3.5 Å to a histidine side-chain during 90% of the simulation time.

It appears that the distribution of water next to individual histidines is not uniform. The histidine on chain A (His-A), interacts with 1–2 water molecules during the first 7 ns but not afterwards. After that, the histidine side-chain rotamer change to further face the lipids so that they lose contact with the water. In contrast, His-B interacts with water for less than 0.2 ns, while His-D only interacts with one water molecule, when the channel structure converges, for a total of ca. 1.5 ns during last 5 ns of the simulation. His-C has

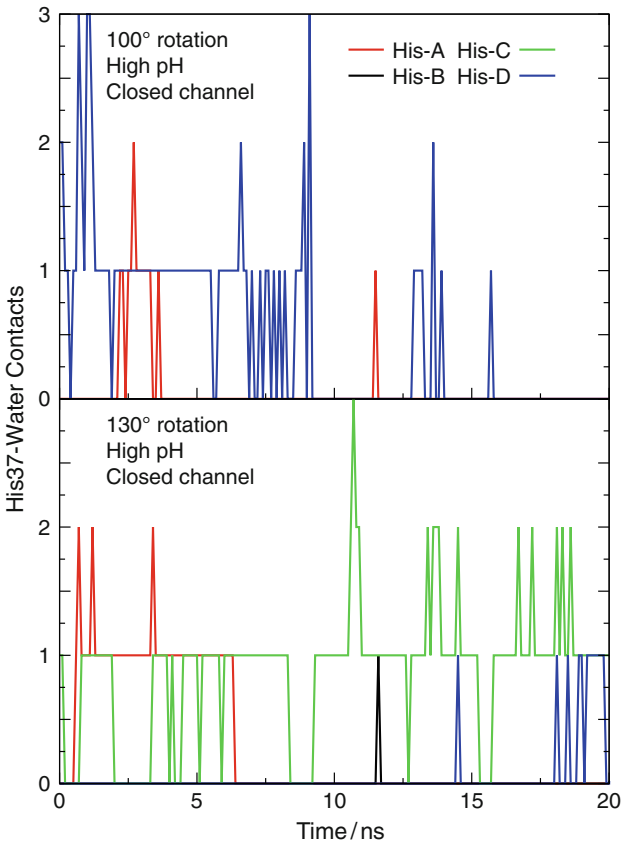

Fig. 4 Number of His37–water contacts (≤3.5 Å) that each of the different systems make, as indicated. The different *lines* represent data for the different histidine residues in the tetramer

the largest number of interactions with water molecules (0–3), spread over nearly the entire simulation, for a total of ca. 16 ns.

For the 100° rotated structure, fewer water–His interactions exist, and most of them disappear in the first half of the simulation. His-A interacts with water molecules for a total of ca. 1.5 ns and in a similar manner to the 130° simulation, it does so only at the beginning of the simulation. His-D interacts with water molecules for a total of 9 ns, during the first 9 ns of the simulation and then again between 12.5 and 16 ns. Both His-B and His-C do not interact with any water molecules for the entire simulation. Despite the fact that this structure appears to converge much faster than the previous one, the dynamics of the water with the protein is variable throughout the production time of this simulation, such that there are fewer interactions in the second half of the simulation.

Conclusions: a mechanism for gating

The recent X-ray structure of M2 (Stouffer et al. 2008) has shown that the channel forms a truncated cone, whereby the N-terminal segment of the channel is tightly packed, and the C-terminal half is widely splayed apart. This finding posed a conundrum, since the only ionizable residues in the channel transmembrane domain, His37 was at the C-terminal half of the transmembrane domain. How then can a change in protonation of His37 results in channel open and closure?

In this study, we have examined the dynamics of an open M2 channel versus a closed channel, according to a model based on FTIR data (Manor et al. 2009). The X-ray structure (Stouffer et al. 2008), with three charged histidine residues, was taken to represent the open channel. A closed channel was generated by rotating the helices of M2 about their individual axes by 100° or 130°, as proposed by a previous study (Manor et al. 2009). In the rotated configurations the polar histidines no longer reside in the channel lumen but rather towards the hydrophobic helix–lipid interface.

It was found that the 130° rotated structure is less stable and takes more time to converge than the 100° rotated structure. Furthermore, both structures have less interactions with water molecules than the open structure, and so they also lose fewer water interactions as the simulation converges. In addition, it was found that the histidines in the 130° structure are oriented in a way that makes them more accessible to water molecules.

One could propose that the histidines face the lipids when they are neutral, while the channel is closed at high pH, but that the interaction of its side-chain with water molecules at low pH is not entirely blocked by its orientation. The histidines may adopt a dihedral angle that enables their side-chain to be within interaction distance from water molecules.

At low pH, such water molecules interactions may result in histidine protonation, thereby creating an unfavorable position for the charged histidines within the lipid bilayer. The charging of the histidines could potentially drive a conformational change that enables the histidines to lock in an "open" orientation while facing the hydrophilic pore. This conformational change would result in channel opening, thereby providing a mechanism for channel gating.

Rotational motion leading to gating, is a feature that is thought to take place in other membrane protein transport systems. For example, both simulations (Sansom 1995; Law et al. 2005) and experiments (Miyazawa et al. 2003; Unwin et al. 2002) propose that the pore lining M2 helices of the acetylcholine receptor, rotate during the course of gating that is controlled by acetylcholine binding. It is noteworthy however that the extent of rotation is still a matter of active research. Finally, two other channel systems that undergo significant rotation upon activation, are the large and small conductance mechanosensitive channels from *Escherichia coli* (Bartlett et al. 2006; Edwards et al. 2005).

Acknowledgments This work was supported in part by grants from the Israeli science foundation (784/01,1249/05,1581/08) to ITA. ITA is the Arthur Lejwa Professor of Structural Biochemistry at the Hebrew University of Jerusalem. Molecular figures were generated by VMD (Humphrey et al. 1996).

References

Bartlett JL, Li Y, Blount P (2006) Mechanosensitive channel gating transitions resolved by functional changes upon pore modification. Biophys J 91(10):3684–3691

Berendsen HJC, Grigera JR, Straatsma TP (1987) The missing term in effective pair potentials. J Phys Chem 91:6269–6271

Berger O, Edholm O, Jahnig F (1997) Molecular dynamics simulations of a fluid bilayer of dipalmitoylphosphatidylcholine at full hydration, constant pressure, and constant temperature. Biophys J 72(5):2002–2013

Brewer ML, Schmitt UW, Voth GA (2001) The formation and dynamics of proton wires in channel environments. Biophys J 80(4):1691–1702

Chen H, Wu Y, Voth GA (2007) Proton transport behavior through the influenza A M2 channel: insights from molecular simulation. Biophys J 93(10):3470–3479

Darden T, York D, Pedersen L (1993) Particle mesh Ewald: an N-log(N) method for Ewald sums in large systems. J Chem Phys 98:10089–10092

Edwards MD, Li Y, Kim S, Miller S, Bartlett W, Black S, Dennison S, Iscla I, Blount P, Bowie JU, Booth IR (2005) Pivotal role of the glycine-rich TM3 helix in gating the MscS mechanosensitive channel. Nat Struct Mol Biol 12(2):113–119

Hay AJ, Kennedy NC, Skehel JJ, Appleyard G (1979) The matrix protein gene determines amantadine-sensitivity of influenza viruses. J Gen Virol 42(1):189–191

Hay AJ, Wolstenholme AJ, Skehel JJ, Smith MH (1985) The molecular basis of the specific anti-influenza action of amantadine. EMBO J 4(11):3021–3024

Hermans J, Berendsen HJC, van Gunsteren WF, Postma JPM (1984) A consistent empirical potential for water–protein interactions. Biopolymers 23:1513–1518

Hess B, Bekker H, Berendsen HJC, Fraaije JGEM (1997) LINCS: a linear constraint solver for molecular simulations. J Comp Chem 18:1463–1472

Hoover WG (1985) Canonical dynamics—equilibrium phase-space distributions. Phys Rev A 31(1):1695–1697

Hu J, Fu R, Nishimura K, Zhang L, Zhou HX, Busath DD, Vijayvergiya V, Cross TA (2006) Histidines, heart of the hydrogen ion channel from influenza A virus: toward an understanding of conductance and proton selectivity. Proc Natl Acad Sci USA 103(18):6865–6870

Humphrey W, Dalke A, Schulten K (1996) VMD—visual molecular dynamics. J Mol Graph 14:33–38

Im W, Feig M, Brooks CL III (2003) An implicit membrane generalized born theory for the study of structure, stability, and interactions of membrane proteins. Biophys J 85(5):2900–2918

Kass I, Arkin IT (2005) How pH opens a H+ channel: the gating mechanism of influenza A M2. Structure 13(12):1789–1798

Law RJ, Henchman RH, McCammon JA (2005) A gating mechanism proposed from a simulation of a human alpha7 nicotinic acetylcholine receptor. Proc Natl Acad Sci USA 102(19):6813–6818

Lear JD (2003) Proton conduction through the M2 protein of the influenza A virus; a quantitative, mechanistic analysis of experimental data. FEBS Lett 552(1):17–22

Lindahl E, Hess B, van der Spoel D (2001) GROMACS 3.0: a package for molecular simulation and trajectory analysis. J Mol Mod 7:306–317

Manor J, Mukherjee P, Lin Y, Leonov H, Skinner JL, Zanni MT, Arkin IT (2009) Gating mechanism of the Influenza A M2 channel revealed by 1 and 2D-IR spectroscopies. Structure 17:247–254

Miyazawa A, Fujiyoshi Y, Unwin N (2003) Structure and gating mechanism of the acetylcholine receptor pore. Nature 423(6943):949–955

Nishimura K, Kim S, Zhang L, Cross TA (2002) The closed state of a H+ channel helical bundle combining precise orientational and distance restraints from solid state NMR. Biochemistry 41(44):13170–13177

Nośe S (1984) A molecular dynamics method for simulations in the canonical ensemble. Mol Phys 52(2):255–268

Nośe S, Klein ML (1983) Constant pressure molecular dynamics for molecular systems. Mol Phys 50:1055–1076

Okada A, Miura T, Takeuchi H (2001) Protonation of histidine and histidine-tryptophan interaction in the activation of the M2 ion channel from influenza a virus. Biochemistry 40(20):6053–6060

Parrinello M, Rahman A (1981) Polymorphic transitions in single crystals: a new molecular dynamics method. J Appl Phys 52:7182–7190

Pinto LH, Holsinger LJ, Lamb RA (1992) Influenza virus M2 protein has ion channel activity. Cell 69(3):517–528

Sakaguchi T, Tu Q, Pinto LH, Lamb RA (1997) The active oligomeric state of the minimalistic influenza virus M2 ion channel is a tetramer. Proc Natl Acad Sci USA 94(10):5000–5005

Sansom MS (1995) Ion-channel gating. Twist to open. Curr Biol 5(4):373–375

Sansom MS, Kerr ID, Smith GR, Son HS (1997) The influenza A virus M2 channel: a molecular modeling and simulation study. Virology 233(1):163–173

Schnell JR, Chou JJ (2008) Structure and mechanism of the M2 proton channel of influenza A virus. Nature 451(7178):591–595

Stouffer AL, Acharya R, Salom D, Levine AS, Di Costanzo L, Soto CS, Tereshko V, Nanda V, Stayrook S, DeGrado WF (2008) Structural basis for the function and inhibition of an influenza virus proton channel. Nature 451(7178):596–599

Takeuchi H, Okada A, Miura T (2003) Roles of the histidine and tryptophan side chains in the M2 proton channel from influenza A virus. FEBS Lett 552(1):35–38

Unwin N, Miyazawa A, Li J, Fujiyoshi Y (2002) Activation of the nicotinic acetylcholine receptor involves a switch in conformation of the alpha subunits. J Mol Biol 319(5):1165–1176

Wang C, Lamb RA, Pinto LH (1995) Activation of the M2 ion channel of influenza virus: a role for the transmembrane domain histidine residue. Biophys J 69(4):1363–1371

Wu Y, Voth GA (2005) A computational study of the closed and open states of the influenza a M2 proton channel. Biophys J 89(4):2402–2411

Yi M, Cross TA, Zhou HX (2008) A secondary gate as a mechanism for inhibition of the M2 proton channel by amantadine. J Phys Chem B 112(27):7977–7979